Using Iterated Extended Kalman Filtering for Estimation of a Hexapod Flight Simulator Motion State

I. Miletović*, D. M. Pool†, O. Stroosma‡, Q. P. Chu§, M. M. Van Paassen¶

The six degrees-of-freedom Stewart platform, or hexapod, is in widespread use in the flight simulation industry for the generation of motion cues that are representative of those experienced in actual flight. For closed-loop control of such motion platforms, but also to be able to objectively assess the quality of the generated simulator motion, accurate measurement of the kinematic state of the motion platform is required. In current practice, the inference of such knowledge relies mainly on the isolated use of actuator length measurements and on, in certain cases, on-platform inertial sensors. The purpose of the current work is to extend a previously proposed and conceptually superior method, based on a tightly-coupled fusion of measurements provided by these sensors using the Iterated Extended Kalman Filter (IEKF). Results from computer simulations indicate that the IEKF has difficulty in converging to the true system state of a six degrees-of-freedom Stewart platform. This is because of the considerable increase in nonlinearity of the platform kinematics. Future research should therefore focus on the application of more advanced filters. In addition, further extension of the sensor fusion scheme using other types of sensors is investigated.

I. Introduction

Modern vehicle simulators used for the purposes of training and research typically rely on various robotic mechanisms to provide a sense of motion similar to that experienced in the real vehicle [1, 2, 3, 4]. The most commonly applied motion platform in flight simulation is the Stewart platform [5], also known as a hexapod system, which consists of a platform supported by six linear actuators moving in a synergistic fashion to provide motion in six degrees-of-freedom (DOF). An example of such a platform is the SIMONA Research Simulator (SRS) at TU Delft, shown in Figure 1. In order to be able to accurately control the motion of the platform (e.g., [6]) and in order to obtain reliable knowledge on the quality of the generated motion cues (e.g., [7, 8]), measuring the kinematic state of the motion platform is of great importance.

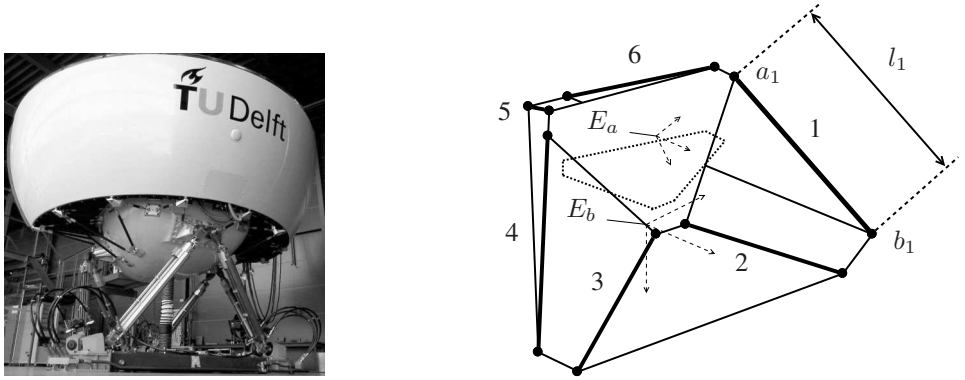

Figure 1. Impression of a Stewart platform used as the motion providing mechanism of the SRS at TU Delft [1].

*Ph.D. Student, Control and Simulation Division, Faculty of Aerospace Engineering, P.O. Box 5058, 2600GB Delft, The Netherlands; i.miletovic@tudelft.nl. Student Member AIAA.

†Assistant Professor, Control and Simulation Division, Faculty of Aerospace Engineering, P.O. Box 5058, 2600GB Delft, The Netherlands; d.m.pool@tudelft.nl. Member AIAA.

‡Researcher, Control and Simulation Division, Faculty of Aerospace Engineering, P.O. Box 5058, 2600GB Delft, The Netherlands; o.stroosma@tudelft.nl. Member AIAA.

§Associate Professor, Control and Simulation Division, Faculty of Aerospace Engineering, P.O. Box 5058, 2600GB Delft, The Netherlands; q.p.chu@tudelft.nl. Member AIAA.

¶Associate Professor, Control and Simulation Division, Faculty of Aerospace Engineering, P.O. Box 5058, 2600GB Delft, The Netherlands; m.m.vanpaassen@tudelft.nl. Senior Member AIAA.

Given the parallel actuators of the Stewart platform, obtaining an accurate estimate of its kinematic state is a well-known challenge [9]. For serial manipulator type mechanisms (e.g., [2]), the position and attitude of the platform can be obtained from the position and attitude of the individual actuators in a straightforward fashion. This relationship is denoted in robotics as the *forward* kinematics. In contrast, the computation of actuators' position and attitude from the position and attitude of the motion platform is known as the *inverse* kinematics. Whereas the latter is easily computed for parallel mechanisms like the Stewart platform, the former, which is more often of interest in practice, is not.

Currently, to compute the forward kinematics of the Stewart platform, measurements of actuator length together with iterative methods such as Newton-Raphson or Gauss-Newton are typically relied upon [10, 6]. These gradient-based methods are applied to arrive at a sufficiently accurate numerical estimate of the position and attitude of the motion platform, given an initial estimate of the position and attitude of the platform. The convergence of such methods not only depends on the initial estimate provided, but also on the geometry of the Stewart platform itself. In addition, although they rely on physical measurements providing the lengths of the six actuators, they lack robustness to measurement inaccuracies. Finally, these methods only provide information on motion platform position and attitude, while often knowledge of the full kinematic state, including velocity and acceleration, is desired. In order to obtain a more complete estimate of the kinematic state of the motion platform without relying on numerical differentiation, actuator length measurements can be complemented with inertial sensors, providing angular rate and specific force [7]. These sensors, however, are known to suffer from significant measurement noise and typically provide biased measurements.

To overcome these issues inherent to the use of multiple isolated sensors with inherent measurement inaccuracies, the use of sensor fusion schemes that rely on the Kalman Filter (KF) [11] are in widespread use in aviation (e.g., [12, 13, 14]). An attempt to apply a similar method for reconstruction of the kinematic state of the Stewart platform has been proposed by Pool et al. in [15]. This work investigated the application of the Extended Kalman Filter (EKF) and Iterated Extended Kalman Filter (IEKF) [16] for the reconstruction of the longitudinal motion states of the Stewart platform. Here, it was found that because of the highly nonlinear nature of the Stewart platform kinematics, the IEKF was required to ensure filter convergence and attain the highly precise state estimates allowed for by the KF approach.

The aim of the current work is to extend the IEKF-based sensor fusion scheme proposed in [15] to all six DOF of the Stewart platform kinematics, which amounts to an even stronger increase in the nonlinearity of the state reconstruction problem. To this end, computer simulations developed using the Python programming language in conjunction with the numerical libraries Numpy, Scipy and Matplotlib [17, 18] are used to implement and subsequently assess the performance of the proposed sensor fusion scheme on the basis of rate of convergence and computational load.

The structure of the paper is as follows. First, a brief background on the theory behind the application of the IEKF-based sensor fusion scheme to the Stewart platform and the extension thereof to the full six DOF is given. Then, the method used to evaluate the IEKF is elaborated upon and, finally, the results of the evaluation are presented.

II. Sensor fusion

The method proposed by Pool et al. in [15] relies on the fusion of measurements from inertial sensors, that is, an Inertial Measurement Unit (IMU) mounted on the Stewart platform, with measurements of the length of each actuator using an extension of the well-known Kalman Filter (KF) to nonlinear systems [11, 16]. A general schematic of the KF is shown in Figure 2.

For a general system, given an initial estimate of its state, denoted by $\underline{\hat{\boldsymbol{x}}}_0$, and its covariance, denoted by P_0, the state as well as the covariance are propagated ahead in time using an internal *linear* model of the stochastic process in conjuction with inputs $\boldsymbol{u}_k$. At the next time instant, when a measurement $\boldsymbol{y}_k$ becomes available, the *prior* estimate of the state, $\underline{\hat{\boldsymbol{x}}}_k^{(-)}$, as well as its covariance, $P_k^{(-)}$, are corrected to obtain the *posterior* state and its covariance, $\underline{\hat{\boldsymbol{x}}}_k^{(+)}$ and $P_k^{(+)}$, respectively. This correction relies on the so-called Kalman gain, K_k, which is selected in the KF in such a way as to minimize the variance of the posterior state estimate:

$$K_k \sim \min_{\underline{\hat{\boldsymbol{x}}}_k^{(+)}} \left[\text{trace} \left(P_k^{(+)} \right) \right] \tag{1}$$

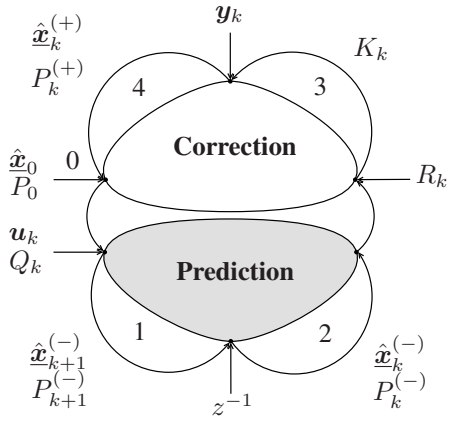

Figure 2. Representation of the Kalman Filter [11].

For the fusion of on-platform inertial sensors with measurements of actuator length in case of the Stewart platform, the inertial sensor measurements are contained in the input vector $\boldsymbol{u}_k$ and are therefore used to propagate the state estimate and its covariance in time. Measurements from the inertial sensors are assumed to be polluted by zero-mean and Gaussian white noise, $\underline{\boldsymbol{w}}$, with covariance Q_k and a constant yet unknown bias, $\underline{\boldsymbol{\lambda}}$. The measurement vector $\boldsymbol{y}_k$ contains the six measured actuator lengths, which are assumed to be polluted by zero-mean and Gaussian white noise, $\underline{\boldsymbol{v}}$, with covariance R_k. This *tightly-coupled* scheme is adopted because it allows all available sensor measurements to be used in their most "raw" form, that is, without application of any form of pre-processing. Any form of pre-processing would result in measurements that are polluted by coloured and correlated noise. As it can be shown that the KF is optimal only in case the measurement noises are zero-mean, white and Gaussian [16, 19], a tightly-coupled sensor fusion scheme is highly advantageous.

A. Stewart platform kinematics

The sensor fusion scheme also relies on an internal mathematical model of the stochastic process. This internal model consists of two parts, a prediction equation that is used to propagate the state estimate ahead in time and an observation equation that is used in the subsequent correction step of the filter. The following nonlinear, time-invariant and stochastic process model can therefore be formulated:

$$\begin{aligned} \dot{\underline{\boldsymbol{x}}}(t) &= f(\underline{\boldsymbol{x}}(t), \boldsymbol{u}(t)) + G(\underline{\boldsymbol{x}}(t))\underline{\boldsymbol{w}}(t) \\ \underline{\boldsymbol{y}}(t) &= h(\underline{\boldsymbol{x}}(t)) + \underline{\boldsymbol{v}}(t) \end{aligned} \tag{2}$$

In case of the Stewart platform, the state vector is chosen to include the position, velocity and attitude of the Upper Gimbal Point (UGP) of the motion platform. The UGP is the centroid of the moving platform of the hexapod system, shown as the origin of reference frame E_a in Figure 1. For reasons of algebraic and numerical convenience, attitude is expressed in terms of the Euler-Rodrigues quaternion formulation [20, 21]. The state vector is furthermore augmented with six inertial sensor biases that are estimated together with the platform states. This approach is common, for example, in the field of aeronautical flight path reconstruction [14] and was also adopted with success in [15]. This brings the total amount of states to sixteen:

$$\boldsymbol{x} = \begin{bmatrix} x & y & z & u & v & w & e_0 & e_x & e_y & e_z & \lambda_x & \lambda_y & \lambda_z & \lambda_p & \lambda_q & \lambda_r \end{bmatrix}^T \tag{3}$$

Given this definition of the state vector, the majority of the prediction equation in Equation (2) follows from basic kinematics and can be obtained in the same fashion as outlined in, e.g., [14]. The quaternion rates can be expressed as follows [20]:

$$\begin{bmatrix} \dot{e}_0 \\ \dot{e}_x \\ \dot{e}_y \\ \dot{e}_z \end{bmatrix} = \frac{1}{2} \begin{bmatrix} -e_x & -e_y & -e_z \\ e_0 & -e_z & e_y \\ e_z & e_0 & -e_x \\ -e_y & e_x & e_0 \end{bmatrix} \begin{bmatrix} p \\ q \\ r \end{bmatrix} \tag{4}$$

In the numerical integration of these rates, normalization of the quaternions needs to be enforced, such that:

$$e_0^2 + e_x^2 + e_y^2 + e_z^2 = 1 \tag{5}$$

The novelty of the sensor fusion scheme proposed in [15], and extended in the current work to all six DOF, lies in the observation equation. Because the measurement vector $\boldsymbol{y}_k$ comprises the six actuator length measurements, the nonlinear function h is expressed as:

$$h(\boldsymbol{x}) = \begin{bmatrix} l_1(\boldsymbol{x}) & l_2(\boldsymbol{x}) & l_3(\boldsymbol{x}) & l_4(\boldsymbol{x}) & l_5(\boldsymbol{x}) & l_6(\boldsymbol{x}) \end{bmatrix}^T \tag{6}$$

where the length of each individual actuator can be derived geometrically as:

$$l_i(\boldsymbol{x}) = \| \boldsymbol{c} + T_{ba}(\boldsymbol{\Phi})\, \boldsymbol{a}_i^a - \boldsymbol{b}_i^b \| \quad \forall \quad i \in [1, \ldots, 6] \tag{7}$$

Here, $\boldsymbol{c}$ and $\boldsymbol{\Phi}$ are the position and attitude vectors of the motion platform, whereas $\boldsymbol{a}_i^{(a)}$ and $\boldsymbol{b}_i^{(b)}$ are the coordinates of the joints of actuator i expressed with respect to reference frame E_a and E_b, respectively (see Figure 1). T_{ba} is the transformation matrix from reference frame E_a to E_b, which is also a function of the attitude of the motion platform. This equation defines the *inverse* kinematics of the Stewart platform and is a severely nonlinear function that depends not only on the position and attitude of the motion platform, but evidently also on the platform geometry. Since the KF relies on a linear stochastic process model and because both the functions f and h are nonlinear, an extension of the KF to nonlinear systems must be applied.

B. Iterated Extended Kalman Filter

A commonly applied nonlinear extension of the KF is the Extended Kalman Filter (EKF) [16]. In the EKF, the nonlinear stochastic process model given by Equation (2) is linearized around a nominal state. This nominal state, in the prediction phase of the filter, is the posterior state estimate $\hat{\underline{\boldsymbol{x}}}_k^{(+)}$ and in the correction phase, is the prior state estimate $\hat{\underline{\boldsymbol{x}}}_k^{(-)}$. As such, the first two terms of the Taylor series expansions of the nonlinear functions f and h, respectively, become:

$$\begin{aligned} f(\underline{\boldsymbol{x}}, \boldsymbol{u}) &\approx f\left(\hat{\underline{\boldsymbol{x}}}_k^{(+)}, \boldsymbol{u}_k\right) + F_k\left(\underline{\boldsymbol{x}} - \hat{\underline{\boldsymbol{x}}}_k^{(+)}\right) \\ h(\underline{\boldsymbol{x}}) &\approx h\left(\hat{\underline{\boldsymbol{x}}}_k^{(-)}\right) + H_k\left(\underline{\boldsymbol{x}} - \hat{\underline{\boldsymbol{x}}}_k^{(-)}\right) \end{aligned} \tag{8}$$

where:

$$F_k = \left.\frac{\partial f(\underline{\boldsymbol{x}}, \boldsymbol{u})}{\partial \underline{\boldsymbol{x}}}\right|_{\underline{\boldsymbol{x}}=\hat{\underline{\boldsymbol{x}}}_k^{(+)}} \qquad \text{and} \qquad H_k = \left.\frac{\partial h(\underline{\boldsymbol{x}})}{\partial \underline{\boldsymbol{x}}}\right|_{\underline{\boldsymbol{x}}=\hat{\underline{\boldsymbol{x}}}_k^{(-)}} \tag{9}$$

These Jacobian matrices are then discretized and applied in the prediction and correction of the estimated state covariance as well as for the computation of the Kalman gain according to the criterium specified in Equation (1).

In [15], it was found that a single application of the correction step illustrated in Figure 2 was insufficient to attain satisfactory convergence of the EKF due to the strongly nonlinear 3-DOF longitudinal kinematics of the Stewart platform in the observation equation. For this reason, the application of the Iterated Extended Kalman Filter (IEKF) was proposed. In the IEKF, the correction step is applied repeatedly at every time instant t_k, each time re-linearizing the nonlinear function h around a temporary iterator, $\hat{\underline{\boldsymbol{\eta}}}_i$, defined by [16]:

$$\hat{\underline{\boldsymbol{\eta}}}_{i+1} = \hat{\underline{\boldsymbol{x}}}_k^{(-)} + K_k\left(\boldsymbol{y}_k - h(\hat{\underline{\boldsymbol{\eta}}}_i, t_k) - H_k\left(\hat{\underline{\boldsymbol{x}}}_k^{(-)} - \hat{\underline{\boldsymbol{\eta}}}_i\right)\right) \tag{10}$$

This iterative correction scheme is also illustrated in Figure 3, from which it can be seen that the state and its covariance improve gradually as multiple iterative corrections are applied. The iterations at each timestep continue until an acceptable improvement threshold, $\epsilon_\eta = \|\hat{\underline{\boldsymbol{\eta}}}_{i+1} - \hat{\underline{\boldsymbol{\eta}}}_i\|_{min}$, is reached or until a maximum number of allowed iterations, N_{max}, is exceeded. Selection of these two parameters is therefore necessary in the application of the IEKF.

For the full 6-DOF kinematics of the Stewart platform, the nonlinearities in the observation equation are even more severe. This is also follows from Equation (7), where it becomes clear that the transformation matrix T_{ba} is more nonlinear when all rotational DOF are included and that these nonlinearities are amplified further upon application of the absolute value. Because of this, the work in the current paper is limited in scope to the evaluation of the IEKF.

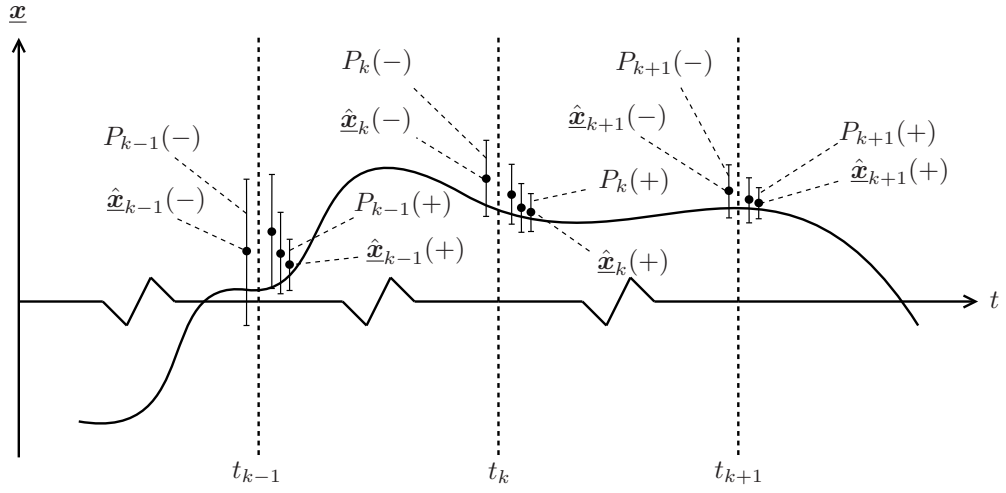

Figure 3. Illustration of the Iterated Extended Kalman Filter.

III. Method

To evaluate the IEKF for reconstruction of the kinematic state of a Stewart platform, a similar approach as the one adopted in [15] is used. Namely, a generic kinematic model of a Stewart platform is defined first and implemented in conjunction with the IEKF. This kinematic model is then used, together with realistic measurement noise levels and biases, to generate artificial sensor data corresponding to a representative motion profile. Subsequently, the adopted initial conditions and other IEKF configuration parameters that are of interest are discussed and, finally, the criteria against which the performance of the IEKF is assessed will be defined.

A. Simulation environment

The computer simulation environment that is used for evaluation of the proposed IEKF-based sensor fusion scheme is developed using the Python programming language, in combination with the open-source numerical and scientific libraries Numpy, Scipy and Matplotlib [17, 18].

The platform on which all simulations are developed comprises a 2.4 GHz Intel® Core^{2}Duo™ processor with eight gigabytes of random access memory. All presented results are furthermore generated with a representative sampling rate of 100 Hz, using the forward Euler method for all numerical integration purposes.

B. Motion platform geometry

The geometry used for the evaluation is that of the SRS, shown in Figure 1. More details regarding the geometry of the SRS are given in Figure 4 and Table 1. Note that l_{min} and l_{max} represent the minimum and maximum length of each actuator. Given r_a, r_b, d_a and d_b it is possible to compute the angles θ_a, θ_b, ξ_a and ξ_b. These, in turn, can be used to compute the coordinates of the actuator joints, $\boldsymbol{a}_i$ and $\boldsymbol{b}_i$, appearing in Equation (7). The gravitional acceleration is assumed to have a magnitude of 9.80665 m/s^2 in the computer simulations.

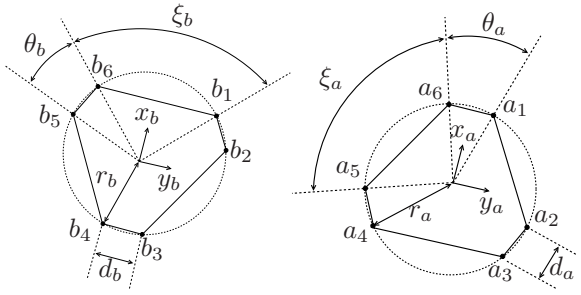

Figure 4. SRS geometry of static base and motion platform.

Table 1. Constants related to the geometry of the SRS.

Constant	Value	Unit
r_a	1.60	m
r_b	1.65	m
d_a	0.20	m
d_b	0.60	m
l_{min}	2.08	m
l_{max}	3.33	m

C. Motion profile

To be able to assess the performance of the IEKF-based sensor fusion scheme, a motion profile must be selected from which to generate the necessary artificial sensor measurements. The motion profile used here is extracted from a recent human-in-the-loop experiment performed on the SRS [22]. In this experiment, subjects were asked to execute a combined roll and pitch tracking task in the presence of both visual and motion cues. This profile was selected because it is representative of typical experiments performed on the SRS.

The trajectory of the motion profile, in terms of a selection of position and attitude time traces, is shown in Figure 5. In addition, a selection of specific forces, angular rates and actuator lengths corresponding to this motion profile are illustrated in Figure 6. In order to preserve space, only the most dominant motion components for the selected motion profile are shown in the current paper.

D. Sensor properties

An important step in the evaluation of the proposed sensor fusion scheme is the introduction of artificial inaccuracies in the simulated inertial sensor and actuator length measurements. The assumed inaccuracies are measurement noise in both sets of measurements and an additional constant bias in the inertial sensor measurements. The noise levels and biases are chosen such that they correspond to the order of magnitude of the noise levels and biases one might find in actual sensory equipment [15].

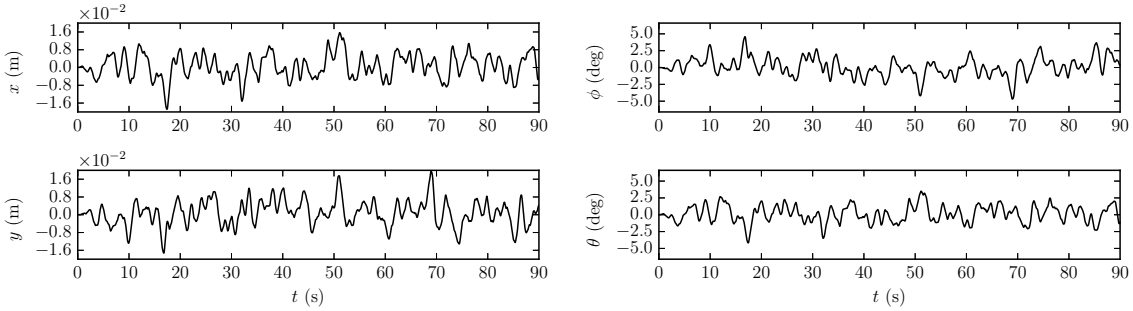

Figure 5. Selected states in trajectory of selected human-in-the-loop experiment performed on the SRS [22].

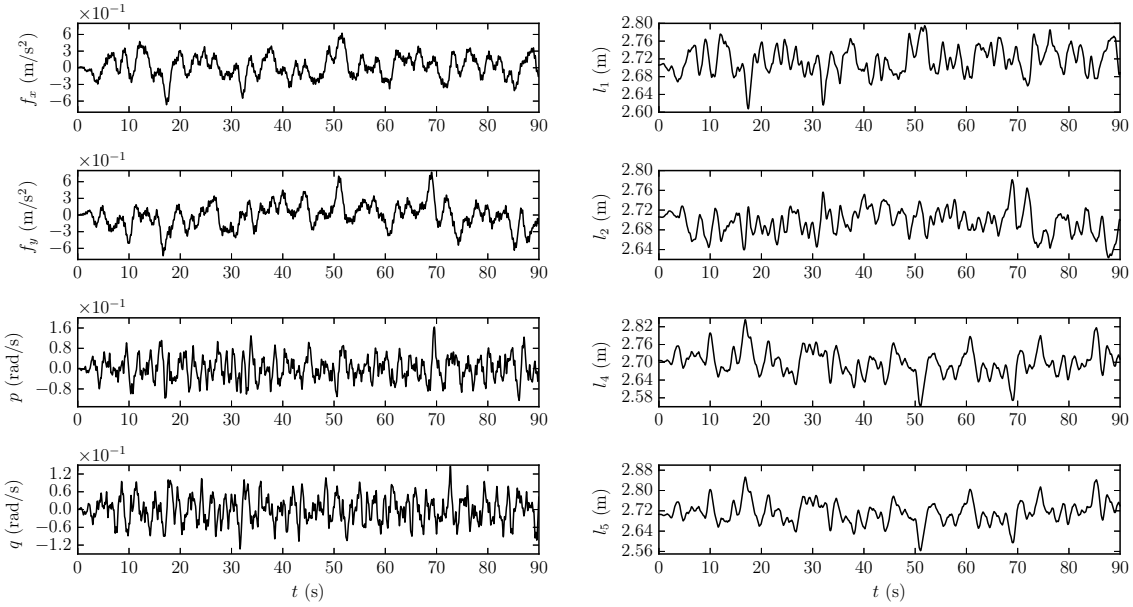

Figure 6. Selection of specific forces (left), rotational rates (left) and actuator lengths (rights) corresponding to selected motion profile [22].

Table 2. Noise standard deviations and bias values superimposed on simulated sensor measurements.

Inertial sensors						Actuator lengths		
σ_{f_x}	$5 \cdot 10^{-3}$	m/s^2	λ_{f_x}	$1 \cdot 10^{-1}$	m/s^2	σ_{l_1}	$1 \cdot 10^{-5}$	m
σ_{f_y}	$5 \cdot 10^{-3}$	m/s^2	λ_{f_y}	$-1 \cdot 10^{-1}$	m/s^2	σ_{l_2}	$1 \cdot 10^{-5}$	m
σ_{f_z}	$5 \cdot 10^{-3}$	m/s^2	λ_{f_z}	$-1 \cdot 10^{-1}$	m/s^2	σ_{l_3}	$1 \cdot 10^{-5}$	m
σ_p	$5 \cdot 10^{-4}$	rad/s	λ_p	$-5 \cdot 10^{-3}$	rad/s	σ_{l_4}	$1 \cdot 10^{-5}$	m
σ_q	$5 \cdot 10^{-4}$	rad/s	λ_q	$5 \cdot 10^{-3}$	rad/s	σ_{l_5}	$1 \cdot 10^{-5}$	m
σ_r	$5 \cdot 10^{-4}$	rad/s	λ_r	$5 \cdot 10^{-3}$	rad/s	σ_{l_6}	$1 \cdot 10^{-5}$	m

The introduced measurement noises are numerically sampled from the standard normal distribution and then scaled such to obtain the standard deviations as listed in Table 2. In case of the inertial sensors, the constant biases also listed in Table 2 are added to the generated measurement noise sequences. A representative selection of the resulting noise sequences and superimposed biases is shown in Figure 7.

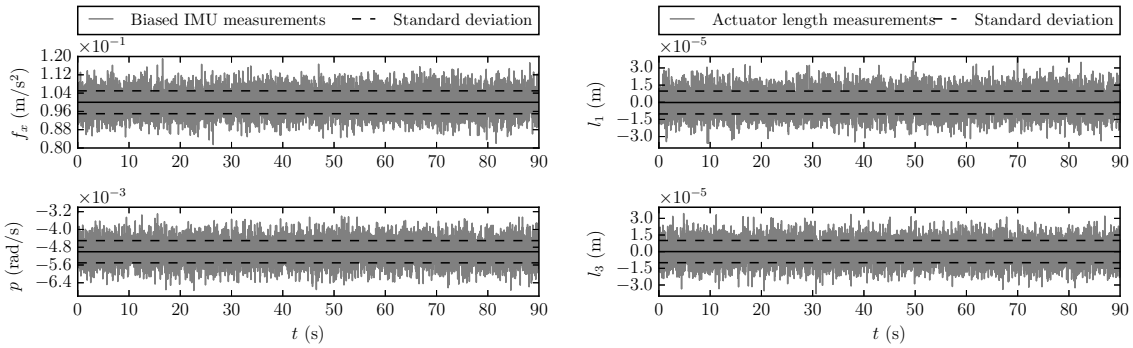

Figure 7. Illustration of measurement inaccuracies inherent in simulated inertial sensors (left) and actuator length measurements (right).

E. IEKF parameter settings and initial conditions

The performance of the IEKF may be controlled with a number of parameters. These are the initial state $\hat{\underline{\boldsymbol{x}}}_0$, the initial state covariance P_0, the measurement noise covariance matrices Q_k and R_k as well as the IEKF-specific parameters, i.e., the improvement threshold ϵ_η and maximum number of allowed iterations N_{max}.

In the current work, the covariance matrices Q_k and R_k are assumed to be time-invariant and diagonal, containing the variances of the measurement noises (see Table 2) on the respective diagonals:

$$Q_k = 1.1 \cdot \text{diag}(\sigma_{f_x}^2, \sigma_{f_y}^2, \sigma_{f_z}^2, \sigma_p^2, \sigma_q^2, \sigma_r^2) \qquad \text{and} \qquad R_k = 1.1 \cdot \text{diag}(\sigma_{l_1}^2, \sigma_{l_2}^2, \sigma_{l_3}^2, \sigma_{l_4}^2, \sigma_{l_5}^2, \sigma_{l_6}^2) \quad (11)$$

The ten percent increase in the magnitude of these matrices is introduced to incorporate some robustness to minor numerical inaccuracies like integration and round-off error.

ϵ_η and N_{max} were assigned the values of $1 \cdot 10^{-6}$ and 1000, respectively. These values are considered conservative and are chosen such to promote increased accuracy and rapid convergence of the filter.

The initial state $\hat{\underline{\boldsymbol{x}}}_0$ and covariance P_0 also influence the rate of convergence of the IEKF. An ititial value for the estimated state that is close to the actual state of the system, in combination with a relatively small magnitude of the initial state covariance, is likely to result in faster convergence. Enlarging the initial state covariance is more likely to result in the exploration of a wider and possibly more nonlinear region of the system dynamics. This may considerably impair rate of convergence. A robust filter should therefore exhibit a fast rate of convergence for a wide selection of initial conditions.

In order to check for this dependency, two initial conditions will be used to evaluate the estimation performance of the proposed sensor fusion scheme:

- *Initial Condition 1 (IC1)*:

$$\begin{aligned} \hat{\underline{\boldsymbol{x}}}_0 &= \begin{bmatrix} 0 & 0 & -2 & 0 & 0 & 0 & 1 & 0 & 0 & 0 & 0 & 0 & 0 & 0 & 0 & 0 \end{bmatrix}^T \\ P_0 &= \text{diag}\left(1^2, 1^2, 1^2, 1^2, 1^2, 1^2, 0.25^2, 0.25^2, 0.25^2, 0.25^2, 0.5^2, 0.5^2, 0.5^2, 0.05^2, 0.05^2, 0.05^2\right) \end{aligned} \quad (12)$$

  This initial condition is representative of a situation where the true state of the system is unknown and therefore specified mostly as zero with a relatively large uncertainty. The exception is the initial estimate for the vertical position of the platform, which is forced to a negative value. This is because of the ambiguity inherent to the Stewart platform, whereby any set of actuator length measurements may correspond to a situation in which the motion platform is either above or below the static base.

- *Initial Condition 2 (IC2)*:

$$\begin{aligned} \hat{\underline{\boldsymbol{x}}}_0 &= \boldsymbol{x}_0 \\ P_0 &= \text{diag}\left((10^{-8})^2, (10^{-8})^2, \ldots, (10^{-8})^2, (10^{-8})^2\right) \end{aligned} \quad (13)$$

This initial condition corresponds to a situation where the true initial state is known to a high accuracy. As such, the initial state covariance is set to approximately zero. Note that, if the initial state covariance would be increased, the value chosen for the initial state estimate is less likely to impact the results significantly. In such cases, the filter will initially perform a type of *random search*. This could result in subsequent estimates that are further away from the true state of the system and would therefore lead to similar results as those obtained for the case of IC1.

F. Evaluation criteria

In order to evaluate the performance of the IEKF-based sensor fusion scheme, the two criteria that will be used are rate of convergence and computational load. Rate of convergence can be evaluated on the basis of how fast the state estimation error converges to zero. However, this quantity can only be obtained for the case of computer simulations, where the true values of the states are known a priori.

In practice, where such information is usually unavailable, a particularly useful quantity that gives valuable insight into the performance of the filter, is the so-called *innovation sequence*. The innovation at any time t_k is defined as:

$$\boldsymbol{\epsilon}_k = \boldsymbol{y}_k - h\left(\hat{\underline{\boldsymbol{x}}}_k^{(-)}\right) \tag{14}$$

As such, the innovation represents the difference between the actual measurement and the output of the observation equation defined in Equation (2) corresponding to the prior state estimate at time t_k. For an optimal filter, it can be shown that the innovation sequence converges to a zero-mean, white and Gaussian signal [19].

Because of these properties, the innovation sequences will be used as the main criteria for assessing the performance of the proposed IEKF-based sensor fusion scheme. During all simulations, required computational time will also be measured to obtain an idea of the impact of the algorithm on the available computational resources.

IV. Results

Figures 8, 9 and 10 show the obtained results for the two initial conditions introduced in Section III.E. These results are a representative sample selected from five consecutive simulation runs performed for both IC1 and IC2. In each run, independently generated noise sequences in accordance with the discussion of Section III.D were introduced.

From these results, it can be deduced that for both cases, the IEKF eventually converges to values close to the true state of the system. The rate of convergence of the states as well as the innovation sequences to those characterizing optimal filter performance is considerably faster for IC2 in comparison to IC1, however. This is an indication that the IEKF has difficulty in coping with the substantial increase in the nonlinearity of the observation equation as compared to the work presented in [15] for the 3-DOF longitudinal kinematics of the Stewart platform.

Another interesting results, for the case of IC1, is the seemingly large estimation error for the quaternions e_x and e_y. This, however, was established to be a direct result of the symmetry inherent in the Euler-Rodrigues quaternion formulation [21]. When the estimated quaternions are converted to their corresponding Euler angle representation, the resulting signals follow a similar trend as those of the other states shown in Figure 9.

In the area of computational load, the required computation time required for each of the two initial conditions was taken as the average value over the five consecutive simulation runs. This resulted in mean computational times of approximately 38 and 30 seconds for IC1 and IC2, respectively, for the 90 second motion profile considered. This difference in computational time between the two conditions is explained by the fact that for the case of IC1, the number of iterative corrections applied as a result of the larger offset and uncertainty in the initial state estimate is also larger. These values are considered acceptable, as the amount of time required to perform the IEKF computations for one timestep are far less than one cycle in a real-time simulation running at a typical rate of 100 Hz [1].

V. Discussion

The results presented in Section IV accurately illustrate the difficulties inherent to the application of the proposed IEKF-based sensor fusion scheme to reconstruct the highly nonlinear 6-DOF kinematics of the Stewart platform. Even though initial conditions can be selected in such a way as to favourably impact the performance of the filter, the fact that the IEKF is highly sensitive to these variations significantly impairs its practical application. In reality, initial conditions are usually not known to an accurate degree and even if they are, occurences of events that in any way disrupt the operation of the filter would require a full re-initialization of the complete system. Filters that are

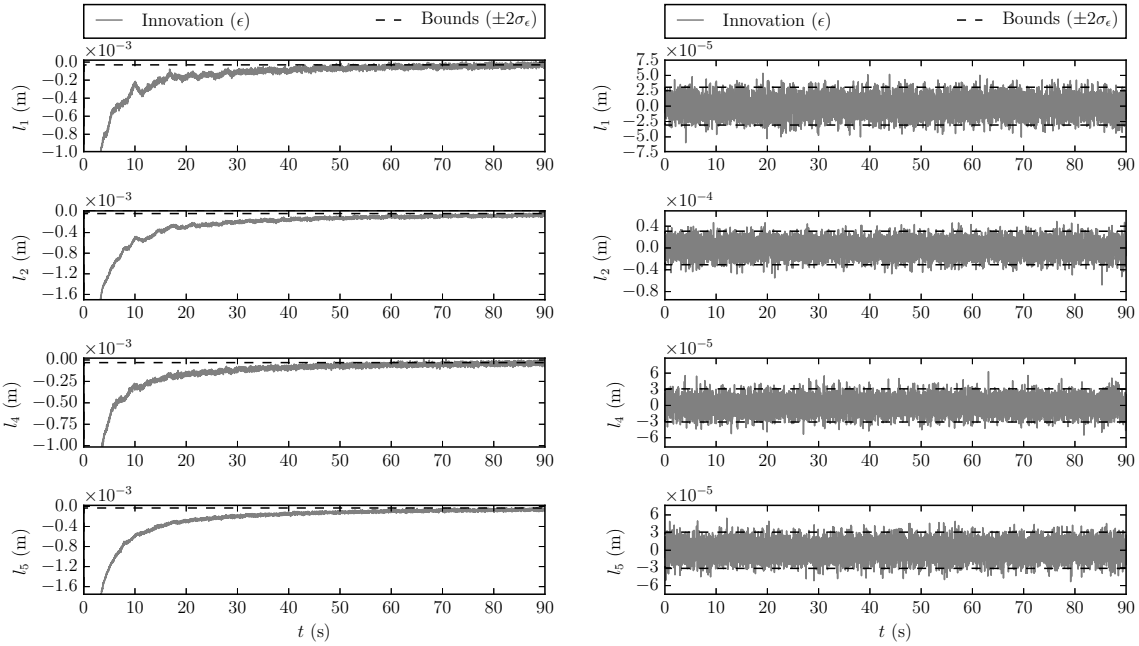

Figure 8. Selection of innovation sequences corresponding to IC1 (left) and IC2 (right).

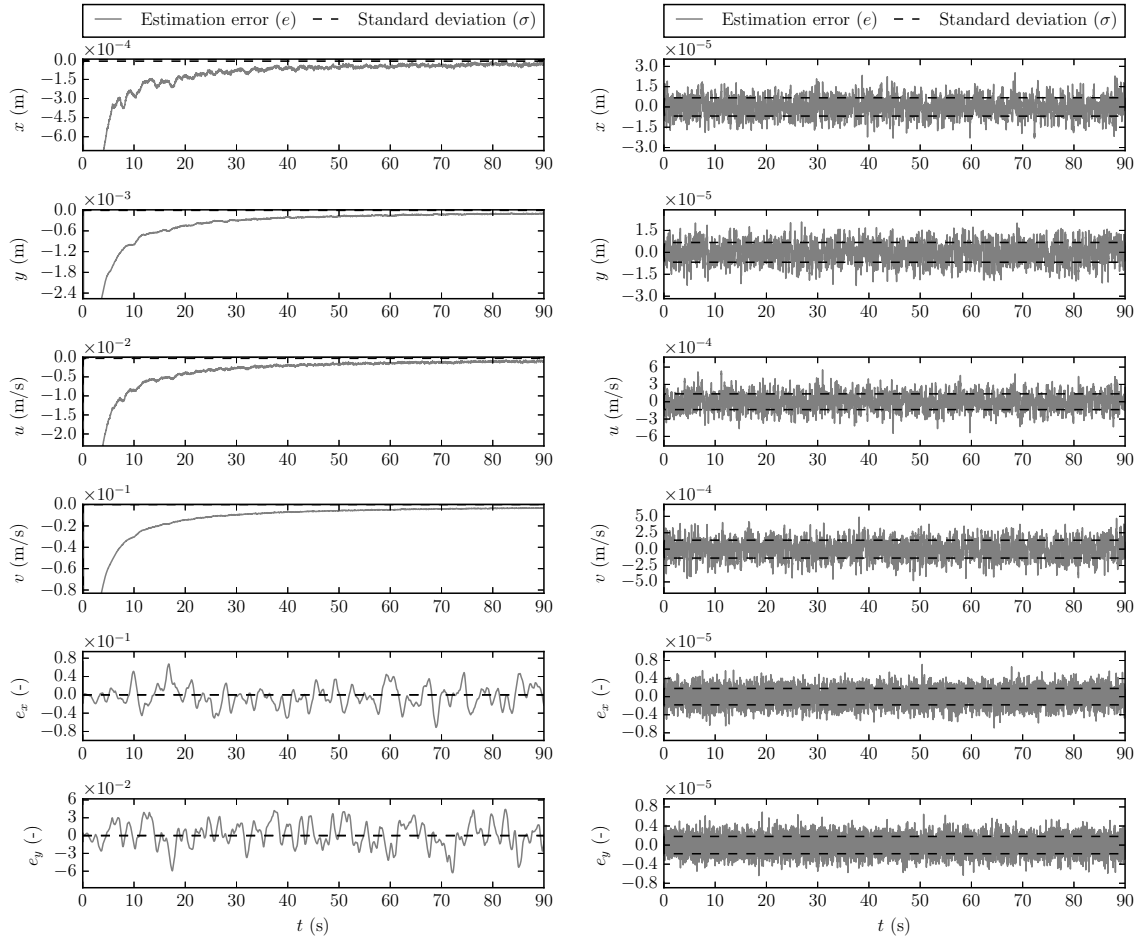

Figure 9. Selection of estimated states corresponding to IC1 (left) and IC2 (right).

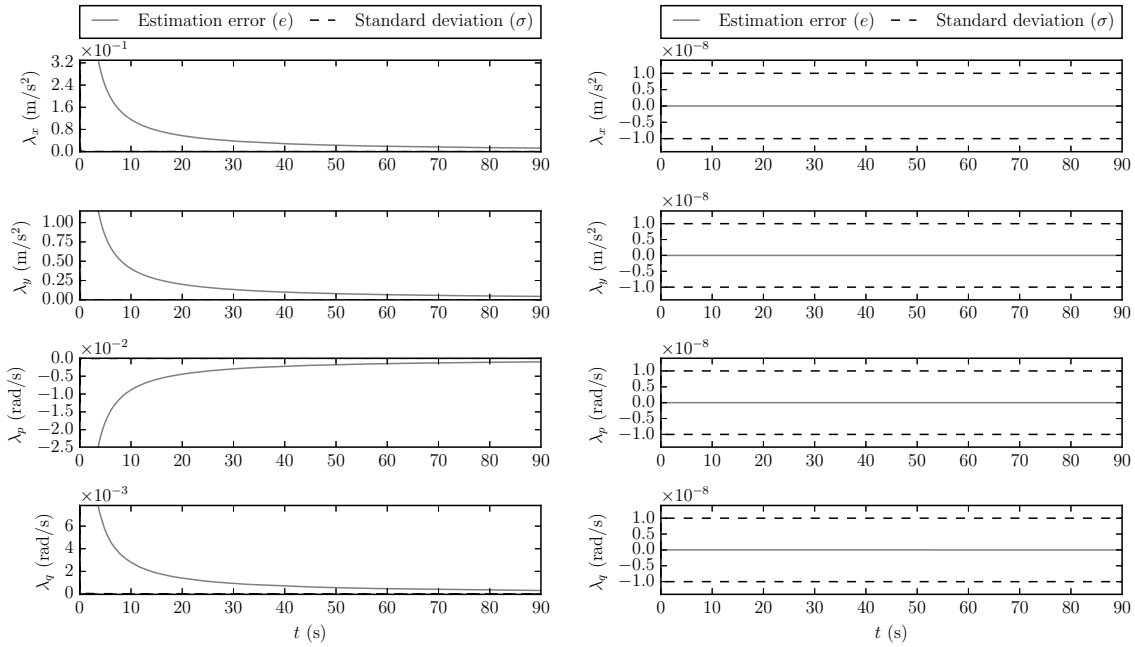

Figure 10. Selection of inertial sensor biases corresponding to IC1 (left) and IC2 (right).

robust to such events would only require an increase of the magnitude of the state covariance matrix to achieve rapid re-convergence of the filter to the new system state.

Nonetheless, the advantages of the proposed sensor fusion scheme as compared to methods in which available sensors are used in isolation remain valid. For one, more information about the kinematic state of the motion platform can be obtained directly (i.e., without numerical differentation), given that velocity is directly estimated. In addition, the inference of inertial sensor biases as part of the sensor fusion scheme facilitates correction of raw measurements, such that unbiased measurements of specific force and rotational rate can be obtained as well. Finally, advances in the development of novel sensory equipment, e.g., angular accelerometers, can be rapidly exploited to extend the state vector and internal mathematical model of the filter to allow direct inference of additional kinematic states.

It is for these reasons that future work on this research topic is focused on the evaluation of more advanced filters, e.g., the Unscented Kalman Filter (UKF) [23], as well as on the incorporation of angular accelerometers. The ability of the UKF to achieve higher order estimation accuracy renders it a prime candidate for application to reconstruction of the highly nonlinear kinematics of the Stewart platform. Furthermore, incorporation of angular accelerometers in the sensor fusion scheme could allow for direct inference of angular rate as well as the ability to obtain unbiased measurements of angular acceleration.

VI. Conclusion

Using the Iterated Extended Kalman Filter (IEKF), a nonlinear extension of the well-known Kalman Filter (KF), the goal of the current work was to evaluate the tightly-coupled fusion of on-platform inertial sensors with actuator length measurements for reconstruction of the kinematic state of a Stewart platform. Previous work in this area was constrained to reconstruction of longitudinal motion states only. This approach has been extended in the current work to the full six degrees-of-freedom of the motion platform.

Computer simulations were developed using the Python programming language to demonstrate the estimation performance of the IEKF for the problem of interest. These simulations revealed a considerable sensitivity of the algorithm to selected initial conditions. The highly nonlinear kinematics of the Stewart platform impaired convergence of the IEKF for an initial condition different from the true initial system state. Such a sensitivity to the selection of initial conditions is undesirable from a practical point of view and should therefore be avoided.

Future research will therefore mainly be devoted to the application of more advanced extensions of the KF to nonlinear systems in order to ensure rapid convergence independent of the selected initial conditions. In addition, the extension of the sensor fusion scheme using other sensors, such as angular accelerometers, will be investigated.

References

[1] Stroosma, O., Van Paassen, M. M., and Mulder, M., "Using The SIMONA Research Simulator For Human-Machine Interaction Research," *AIAA Modeling and Simulation Technologies Conference and Exhibit, Austin, Texas, Aug. 11-14*, No. AIAA-2003-5525, 2003, pp. 1–8.

[2] Teufel, H. J., Nusseck, H.-G., Beykirch, K. A., Butler, J. S., Kerger, M., and Bülthoff, H. H., "MPI Motion Simulator: Development and Analysis of a Novel Motion Simulator," *Proceedings of the AIAA Modeling and Simulation Technologies Conference and Exhibit, Hilton Head (SC)*, No. AIAA-2007-6476, 2007.

[3] Zaal, P. M. T., Schroeder, J. A., and Chung, W. W. Y., "Transfer of Training on the Vertical Motion Simulator," *Proceedings of the AIAA Modeling and Simulation Technologies Conference, Atlanta (GA)*, No. AIAA-2014-2206, June 2014.

[4] Wentink, M., Valente Pais, A. R., Mayrhofer, M., Feenstra, P., and Bles, W., "First Curve Driving Experiments in the Desdemona Simulator," *Driving Simulation Conference Europe, Monaco, 31 January, 1 February 2008*, Feb. 2008, pp. 135–146.

[5] Stewart, D., "A Platform with Six Degrees of Freedom," *Proceedings of the Institution of Mechanical Engineers*, Vol. 180, No. 1, 1965, pp. 371–386.

[6] Koekebakker, S. H., *Model Based Control of Flight Simulator Motion Bases*, Ph.D. thesis, Delft University of Technology, 2001, `http://repository.tudelft.nl/view/ir/uuid%3Aeccd2fa5-e4f1-43ff-b074-3d6245fa24b9/`.

[7] Berkouwer, W. R., Stroosma, O., van Paassen, M. M., Mulder, M., and Mulder, J. A., "Measuring the Performance of the SIMONA Research Simulator's Motion System," *Proceedings of the AIAA Modeling and Simulation Technologies Conference and Exhibit, San Francisco, California, Aug. 15-18*, No. AIAA 2005-6504, 2005, pp. 1–12.

[8] Stroosma, O., van Paassen, M. M., Mulder, M., Hosman, R. J. A. W., and Advani, S. K., "Applying the Objective Motion Cueing Test to a Classical Washout Algorithm," *Proceedings of the AIAA Modeling and Simulation Technologies Conference, Boston (MA)*, No. AIAA-2013-4834, Aug. 2013.

[9] Dasgupta, B. and Mruthyunjayab, T. S., "The Stewart Platform Manipulator: A Review," *Mechanism and Machine Theory*, Vol. 35, 2000, pp. 15–40.

[10] Dieudonne, J. E., Parrish, R. V., and Bardusch, R. E., "An Actuator Extension Transformation for a Motion Simulator and an Inverse Transformation applying Newton-Raphson's Method," Tech. Rep. D-7067, NASA, 1972.

[11] Kalman, R. E., "A New Approach to Linear Filtering and Prediction Problems," *Transactions of the ASME, Journal of Basic Engineering*, Vol. 82, No. Series D, 1960, pp. 35–45.

[12] Jonkers, H. L., "Application of the Kalman Filter to Flight Path Reconstruction from Flight Test Data Including Estimation of Instrumental Bias Error Corrections," Tech. Rep. VTH-162, Delft University of Technology, Faculty of Aerospace Engineering, 1976, `http://repository.tudelft.nl/view/ir/uuid%3A93c3dd1c-c96f-458a-a2c2-c924c9fe898a/`.

[13] Horsten, J. J., Jonkers, H. L., and Mulder, J. A., "Flight Path Reconstruction in the Context of Nonsteady Flight Testing," Tech. Rep. LR-280, Delft University of Technology, Faculty of Aerospace Engineering, 1979, `http://repository.tudelft.nl/view/ir/uuid%3A240c1a7c-1bce-46d5-9df4-0df67a4d148d/`.

[14] Mulder, J. A., Chu, Q. P., Sridhar, J. K., Breeman, J. H., and M. Laban, "Non-Linear Aircraft Flight Path Reconstruction: Review and New Advances," *Progress in Aerospace Sciences*, Vol. 35, No. 7, 1999, pp. 673–726.

[15] Pool, D. M., Chu, Q. P., Mulder, M., and van Paassen, M. M., "Optimal Reconstruction of Flight Simulator Motion Cues using Extended Kalman Filtering," *Proceedings of the AIAA Modeling and Simulation Technologies Conference and Exhibit, Honolulu, Hawai, Aug. 18-21*, No. AIAA-2008-6539, 2008.

[16] Gelb, A., *Applied Optimal Estimation*, The M.I.T. Press, 1974.

[17] Oliphant, T. E., "Python for Scientific Computing," *Computing in Science and Engineering*, Vol. 9, No. 3, 2007.

[18] Hunter, J. D., "Matplotlib: A 2D Graphics Environment," *Computing in Science and Engineering*, Vol. 9, No. 3, 2007.

[19] Anderson, B. D. O. and Moore, J. B., *Optimal Filtering*, Prentice Hall Information and System Sciences Series, 1979.

[20] Phillips, W. F. and Hailey, C. E., "Review of Attitude Representations Used for Aircraft Kinematics," *Journal of Aircraft*, Vol. 38, No. 4, 2001, pp. 718–737.

[21] Soijer, M. W., "Rotations as Double Reflections and Geometrical Derivation of Euler-Rodrigues Parameters," *AIAA Journal of Guidance, Control and Dynamics*, Vol. 32, No. 1, 2009, pp. 313–318.

[22] Zaal, P. M. T. and Pool, D. M., "Multimodal Pilot Behavior in Multi-Axis Tracking Tasks with Time-Varying Motion Cueing Gains," *Proceedings of the AIAA Modeling and Simulation Technologies Conference, National Harbor, Maryland, Jan. 13-17*, No. AIAA-2014-0810, 2014.

[23] S. J. Julier and J. K. Uhlmann, "A New Extension of the Kalman Filter to Nonlinear Systems," *Proceedings of the International Symposium on Aerospace/Defence Sensing, Simulation and Controls, Orlando, Florida, Apr. 20-25*, 1997, pp. 182 – 193.